SUPPLEMENTARY INFORMATION

Two-dimensional Cu-phenylalanine nanoflakes for efficient and robust CO_2 electroreduction to C_{2+} products

Wenda Zhou,[a, b] Mingyue Chen,[c] Xingfang Luo,[b] Cailei Yuan,[b]* Shoujie Liu,[a] Wen Lei,[c] and Shouguo Wang[a, c]*

[a] Anhui Provincial Key Laboratory of Magnetic Functional Materials and Devices, School of Materials Science and Engineering, Anhui University, Hefei 230601, 111 Jiulong Road, Anhui, China

[b] Key Laboratory of Green Hydrogen and Advanced Catalysis of Jiangxi Province, School of Physics, Communication and Electronics, Jiangxi Normal University, 99 Ziyang Avenue, Nanchang 330022, Jiangxi, China

[c]School of Materials Science and Engineering, Beijing Advanced Innovation Center for Materials Genome Engineering, University of Science and Technology Beijing, 30 Xueyuan Road, Haidian District, Beijing 100083, China

[d]Department of Electrical, Electronic and Computer Engineering, The University of Western Australia, 35 Stirling Highway, Crawley, 6009, Australia

* Corresponding author. E-mail: clyuan@jxnu.edu.cn, ORCID:0000-0002-8088-0313. sgwang@ahu.edu.cn.

Keywords: CO_2 reduction; C−C coupling; coordination compounds; moderate oxidation state

Experimental section

Synthesis of samples: 50 mL $CuCl_2$ (5 mM, 99%, sigma-aldrich) aqueous solution was slowly added to 100 mL L-phenylalanine (10 mM, 99%, sigma-aldrich) solution (containing NaOH (10 mM, 98%, sigma-aldrich)) under heating (60 °C). Thin crystals were groweded at the liquid–air interface. The obtained crystals are filtered out and washed with deionized water, followed by vacuum drying in a freeze dryer.

Material characterizations: For single-crystal XRD characterization, the crystals suitable for test were coated with Paratone oil (Hampton Research) and mounted on a MiTeGen loops and flash frozen in liquid nitrogen. The prepared crystals were measured by a Rigaku XtaLabPro full Kappa diffractometer. Data were collected and processed with CrysAlis^{Pro}. The temperature was set at 193 K using nitrogen flow. The X-ray crystallographic coordinates for samples are available from the Cambridge Crystallographic Data Centre (CCDC), under deposition number CCDC 1871975 for Cu-phe. X-ray absorption fine structure (XAFS) spectroscopy was carried out using the RapidXAFS 2M (Anhui Absorption Spectroscopy Analysis Instrument Co., Ltd.) by transmission (or fluorescence) mode at 20 kV and 20 mA. The XAFS data were processed using the ATHENA module implemented in the IFEFFIT software packages, and the least-square curve-fitting was accomplished by using the ARTEMIS module of IFEFFIT.

Electrochemical measurements: A catalyst (10.0 mg) and carbon powder (0.1 mg) were dispersed in a mixture including 960 μL of ethanol and 80 μL of Nafion to form homogeneous ink after ultrasonication. Next, 200 μL of the catalyst ink was spread onto glassy carbon flat surface (1 cm^2) and then dried in vacuum drying chamber. The

loading of the catalyst was 2 mg cm^{-2}. Electrochemical characterizations were characterized by using a electrochemical workstation (CHI 760) and a gas-tight H-type cell. Two chambers in the reactor were separated by a Nafion-117 membrane. Cu-phe deposited on a glassy carbon flat as working electrodes, a platinum plate as counter electrode and a saturated Hg/HgCl electrode as reference electrode. The electrolyte (0.5 M KHCO3) was bubbled with Ar or CO_2 for more than 30 min to form an Ar-saturated or a CO_2-saturated solution. Liquid products were quantified by nuclear magnetic resonance (NMR, Agilent 600 MHz), gas-phase products were detected by the on-line analysis though gas chromatograph (Agilent 8860). NMR tubes were prepared by combining 630 μL of samplewith 70μL D_2O and 30μL of aqueous 5mM DMSO internal standard. The Faraday efficiency (FE) of gas products is calculated as follows: FE=NFyVP/IRT. Where N is the number of electrons required for the product (N is equal to 12 for C_2H_4), and y is the volume concentration of the gas product. V is the gas flow rate at room temperature and ambient pressure. I is the steady-state measurement current. The constant is as follows: P = 1.013×10^5 Pa, T = 298.15 K, F = 96485 $Cmol^{-1}$, R = 8.3145 $Jmol^{-1}K^{-1}$. FE of liquid products is calculated as follows: $FE=NFn_{product}/Q$. $n_{product}$ denotes the moles of the obtained formate calculated by NMR, Q denotesthe total charge. For flow cell test, a gas-tight, customized three-chamber flow cell (Gaoss Union) was used to conduct electrochemical reaction. A Nafion-117 membrane was used to conduct ions and separate the catholyte and anolyte chambers. The platinum plate and a saturated Hg/HgCl electrode were used as the counter and reference electrode, respectively. 0.5 M $KHCO_3$ was used as the electrolyte. The CO_2 flow rate was 40 sccm, controlled by a mass flow meter. The catalyst ink was spread onto Sigracet 29 BC gas diffusion electrode (GDE) and the loading of the catalyst still was 2 mg cm^{-2}.

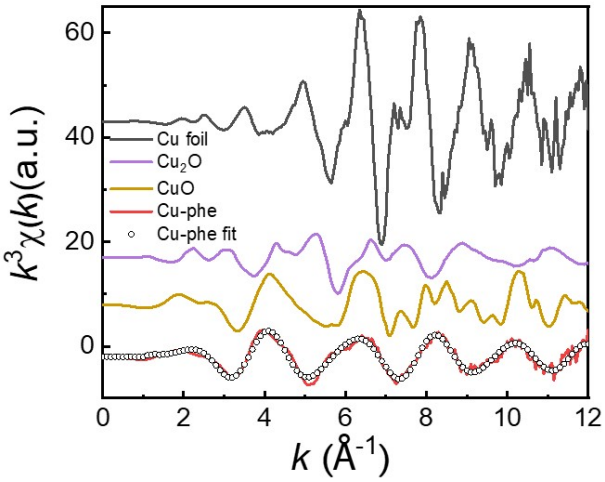

Figure S1. Cu K-edge $k^3\chi(k)$ functions of Cu foil, Cu-phe nanoflakes, Cu_2O and CuO.

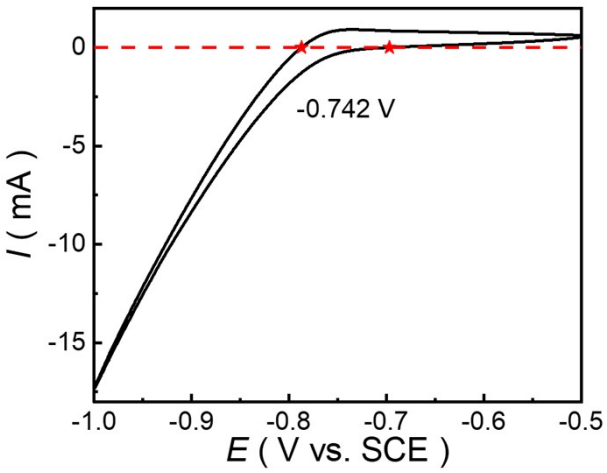

Figure S2. Reference electrode calibration curve.

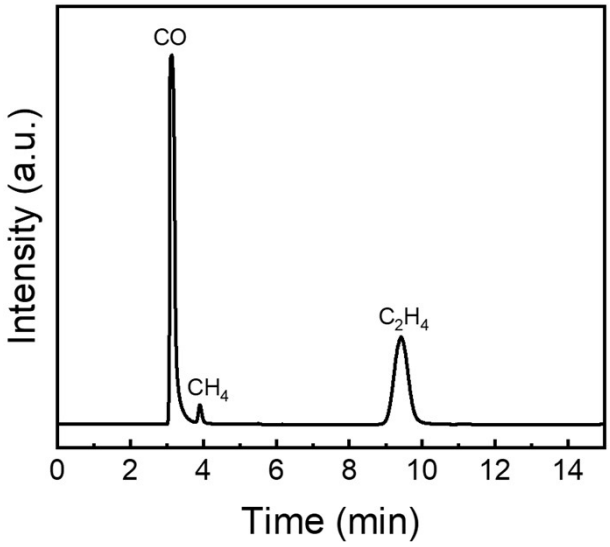

Figure S3. Representative gas chromatography (GC) flame ionization detector (FID) spectrum for CO_2RR products.

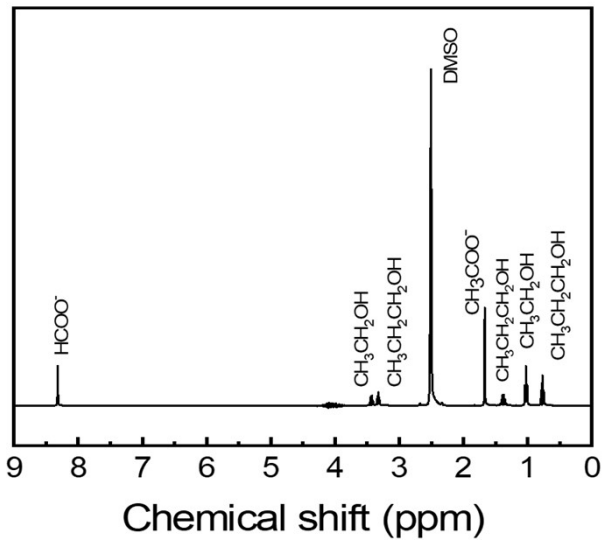

Figure S4. Representative NMR spectrum for CO_2RR products.

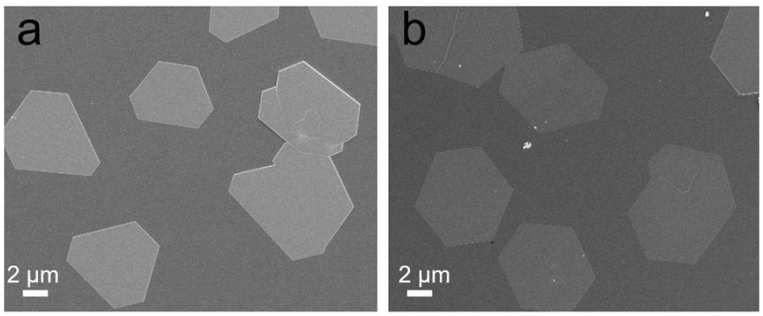

Figure S5. SEM images of Cu-phe nanoflakes before (a) and after (b) electrocatalytic tests.

Supplementary Table

Table S1 | Selected some high-performance electrocatalysts for CO_2RR reported in the literature. In H-cell reactor (H); In flow cell reactor (F).

Catalysts	Potential [V vs. RHE]	FE C_{2+}	Electrolytes	Current Density (mA/ cm^2)	Ref.
Cu-phe (H)	-0.8	81.3%	0.5 M $KHCO_3$	-22.07	This work
Cu-phe (F)	-0.8	88.1%	0.5 M $KHCO_3$	-87.79	This work
Cu_v-Cu_2O	-1.3	30.48%	0.5 M $KHCO_3$	≈-50	[1]
B-Cu_xO (H)	-1.0	48.44%	0.5 M $KHCO_3$	≈-33	[2]
CeO_2/CuS	-0.5	51.2%	0.1 M $KHCO_3$	≈-6	[3]
P-Cu	-1.3	57.22	0.1 M $KHCO_3$	-18	[4]
$Pd^{\delta-}$–$Cu^{\delta+}$(F)	-1.5	78.2	1 M KOH	-116.1	[5]
OD-Cu-200(H)	-0.95	61.5	0.5 M $KHCO_3$	≈-30	[6]
$Cu_2(OH)_2CO_3$ (H)	-1.55	76.29%	0.1 M $KHCO_3$	-20	[7]
$Cu_{9.77}/CeO_2$ (H)	-1.0	78.36%	0.1 M CsI	-16.8	[8]
CuBtz (H)	-1.3	73.7%	0.1 M $KHCO_3$	-7.9	[9]
S-HKUST-1 (H)	−1.32	60.0%	0.1 M $KHCO_3$	-19.1	[10]
Branched Cu	-1.08	70%%	0.1 M $KHCO_3$	-27.5	[11]
Cu_3-Br	-0.7	55%	0.5M KOH	-129.58	[12]
KB@$Cu_3(HITP)_2$	-1.37	70%	0.1 M $KHCO_3$	-25	[13]
Cu_2O@HKUST-1	-1.08	68%	0.1 M $KHCO_3$	-5	[14]
Plasma Cu nanocubes	-1.0	73%	0.1 M $KHCO_3$	35.2	[15]

References

[1] Sun, Y., Wang, X., Zhang, H., Gao, X., Wang, X., Wang, S., Yan, Y. M. (2024). Deciphering the Stability Mechanism of Cu Active Sites in CO_2 Electroreduction via Suppression of Antibonding Orbital Occupancy in the O 2p-Cu 3d Hybridization. ACS Catalysis, 2024, 14, 1351-1362.

[2] Yang, C., Wang, R., Yu, C., Xiao, J., Huang, Z., Lv, B., Zhao, H., Wu, X., Jing, G. et al. Engineering stable Cu^{+}-Cu^{0} sites and oxygen defects in boron-doped copper oxide for electrocatalytic reduction of CO_2 to C_{2+} products. Chemical Engineering Journal, 2024, 484, 149710.

[3] Yang, Z., Ji, D., Li, Z., He, Z., Hu, Y., Yin, J., Yan, C. H. CeO_2/CuS nanoplates electroreduce CO_2 to ethanol with stabilized Cu^{+} species. Small, 2023, 19, 2303099.

[4] B. Liu, C. Cai, B.P. Yang, K.J. Chen, Y. Long, Q.Y. Wang, S.D. Wang, G.Z. Chen, H.M. Li, J.H. Hu, J.W. Fu, M. Liu, Intermediate enrichment effect of porous Cu catalyst for CO_2 electroreduction to C_2 fuels, Electrochim. Acta, 2021, 388, 138552.

[5] Zhang, Z., Chen, S., Zhu, J., Ye, C., Mao, Y., Wang, B. Charge-Separated $Pd^{\delta-}$–$Cu^{\delta+}$ Atom Pairs Promote CO_2 Reduction to C_2. Nano Letters, 2023, 23, 2312-2320.

[6] Wei D, Wang Y, Dong C L, et al. Surface Adsorbed Hydroxyl: A Double‐Edged Sword in Electrochemical CO_2 Reduction over Oxide-Derived Copper. Angewandte Chemie International Edition, 2023, 62, e202306876.

[7] He X, Wang M, Wei Z, et al. Dual‐Anion‐Stabilized $Cu^{\delta+}$ Sites in $Cu_2(OH)_2CO_3$ for High C_{2+} Selectivity in the CO_2 Electroreduction Reaction. ChemSusChem, 2024, e202400871.

[8] Fang M, Xia W, Han S, et al. Boosting CO_2 Electroreduction to Multi‐carbon Products via Oxygen‐rich Vacancies and Ce^{4+}– O_2– Cu^+ Structure in Cu/CeO_2 for Stabilizing Cu^+[J]. ChemCatChem, 2024, 16, e202301266.

[9] H.L. Zhu, H.Y. Chen, Y.X. Han, Z.H. Zhao, P.Q. Liao, X.M. Chen, A Porous pi-pi Stacking Framework with Dicopper(I) Sites and Adjacent Proton Relays for Electroreduction of CO_2 to C_{2+} Products, J. Am. Chem. Soc. 2022, 144, 13319–13326.

[10] Wen, C. F.; Zhou, M.; Liu, P. F.; Liu, Y.; Wu, X.; Mao, F.; Dai, S.; Xu, B.; Wang, X. L.; Jiang, Z.; et al. Highly ethylene-selective electrocatalytic CO_2 eduction enabled by isolated Cu-S motifs in metal-organic framework based precatalysts. Angew. Chem., Int. Ed. 2022, 61, e202111700.

[11]Kim, J.; Choi, W.; Park, J. W.; Kim, C.; Kim, M.; Song, H., Branched Copper Oxide Nanoparticles Induce Highly Selective Ethylene Production by Electrochemical Carbon Dioxide Reduction. J. Am. Chem. Soc. 2019, 141, 6986-6994.

[12]Kim, J.; Choi, W.; Park, J. W.; Kim, C.; Kim, M.; Song, H., Branched Copper Oxide Nanoparticles Induce Highly Selective Ethylene Production by Electrochemical Carbon Dioxide Reduction. J. Am. Chem. Soc. 2019, 141, 6986-6994.

[13]Sun, H.; Chen, L.; Xiong, L.; Feng, K.; Chen, Y.; Zhang, X.; Yuan, X.; Yang, B.; Deng, Z.; Liu, Y.; Rummeli, M. H.; Zhong, J.; Jiao, Y.; Peng, Y., Promoting ethylene production over a wide potential window on Cu crystallites induced and stabilized via current shock and charge delocalization. Nat. Commun. 2021, 12, 6823.

[14]Tan, X.; Yu, C.; Zhao, C.; Huang, H.; Yao, X.; Han, X.; Guo, W.; Cui, S.; Huang, H.; Qiu, J., Restructuring of Cu_2O to Cu_2O@Cu-Metal-Organic Frameworks for Selective Electrochemical Reduction of CO_2. ACS Appl Mater Interfaces 2019, 11, 9904-9910.

[15]Gao, D.; Zegkinoglou, I.; Divins, N. J.; Scholten, F.; Sinev, I.; Grosse, P.; Roldan Cuenya, B., Plasma-Activated Copper Nanocube Catalysts for Efficient Carbon Dioxide Electroreduction to Hydrocarbons and Alcohols. ACS Nano 2017, 11, 4825-4831.